

Accepted Manuscript

Enhanced antibacterial activity of Egyptian local insects' chitosan-based nanoparticles loaded with ciprofloxacin-HCl

Narguess Marei, Ahmed H.M. Elwahy, Taher A. Salah, Youssef El Sherif, Emtithal Abd El-Samie



PII: S0141-8130(18)33703-6
DOI: <https://doi.org/10.1016/j.ijbiomac.2018.12.204>
Reference: BIOMAC 11363

To appear in: *International Journal of Biological Macromolecules*

Received date: 19 July 2018
Revised date: 11 December 2018
Accepted date: 21 December 2018

Please cite this article as: Narguess Marei, Ahmed H.M. Elwahy, Taher A. Salah, Youssef El Sherif, Emtithal Abd El-Samie , Enhanced antibacterial activity of Egyptian local insects' chitosan-based nanoparticles loaded with ciprofloxacin-HCl. *Biomac* (2018), <https://doi.org/10.1016/j.ijbiomac.2018.12.204>

This is a PDF file of an unedited manuscript that has been accepted for publication. As a service to our customers we are providing this early version of the manuscript. The manuscript will undergo copyediting, typesetting, and review of the resulting proof before it is published in its final form. Please note that during the production process errors may be discovered which could affect the content, and all legal disclaimers that apply to the journal pertain.

Title:

Enhanced antibacterial activity of Egyptian Local insects' chitosan-based nanoparticles loaded with ciprofloxacin-HCl

Authors:

Narguess Marei¹, Ahmed H. M. Elwahy¹, Taher A. Salah², Youssef El Sherif³, Emtithal Abd El-Samie^{4*}

Affiliations:

¹Chemistry Department, Faculty of Science, Cairo University, Giza, Egypt.

²Nanotechnology Research Centre, British University in Egypt, Cairo, Egypt.

³Department of pharmaceutics and drug technology, Faculty of Pharmacy, Heliopolis University, Cairo Egypt.

⁴Entomology Department, Faculty of Science, Cairo University, Giza, Egypt.

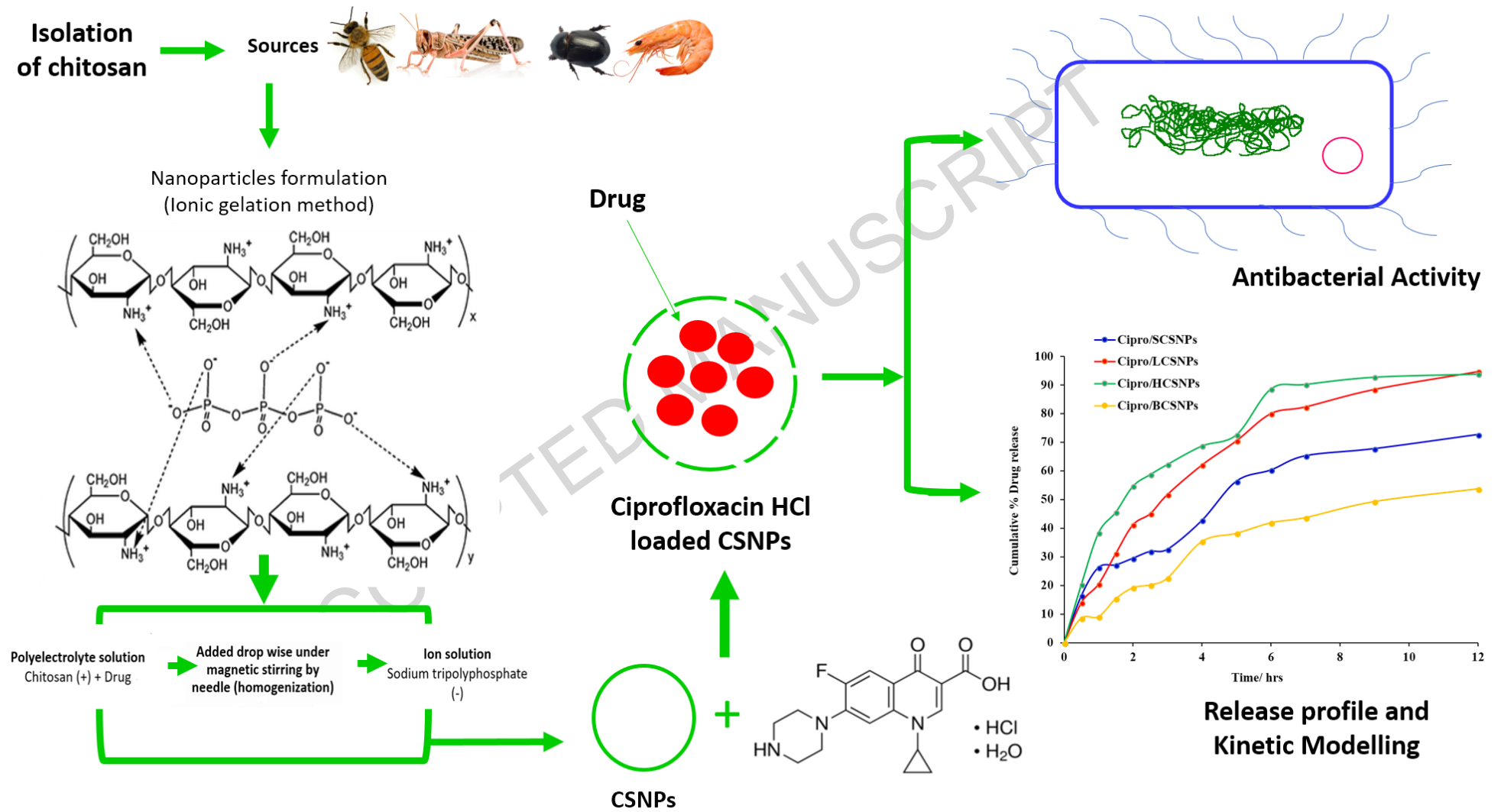
*Corresponding author: Emtithal_a@yahoo.com

Abstract:

Chitosan (CS), possess enormous properties, being biodegradable, biocompatible, and antimicrobial. CS could be formulated and casted into different forms including 2D films, hydrogels, and nanoparticles. Chitosan-based nanoparticles (CSNPs) showed countless interest as polymeric drug delivery system (DDS) with its improved bioavailability, and stability when compared with traditional DDS. Ciprofloxacin is a prescribed antibiotic for many diseases, but its efficiency was affected by antibacterial resistance. Therefore, in this study, CSNPs loaded with ciprofloxacin (Cipro/CSNPs) were prepared from CS isolated from desert locusts, beetles, honey bee exoskeletons, and shrimp shells were used as a standard control. CSNPs were formulated by ionic crosslinking method, then loaded with ciprofloxacin HCl, and characterized using particle size distribution, zeta potential, and drug entrapment efficiency. The release of ciprofloxacin from CSNPs was evaluated and its kinetic modelling was performed. Antibacterial activity of CSNPs was evaluated against *Escherichia coli*, *Bacillus thuringiensis*, Methicillin-resistant *Staphylococcus aureus* (MRSA) and, *Pseudomonas aeruginosa*. Minimum inhibitory concentrations (MIC) were determined and compared between chitosan sources. The Cipro/CSNPs results indicate that the highest antibacterial activity against *E. coli* and MRSA with MIC varying from 0.0043 to 0.01 µg/ml and from 0.07 to 0.14 µg/ml, respectively. In addition, CSNPs enhanced drug delivery, and allowed its controlled release.

Key words: Chitosan nanoparticles; antibacterial activity; drug delivery.

Graphical abstract:



1. Introduction:

The biodegradable polymer chitosan [(1, 4) -2- amino-2-deoxy-D-glucan] is a linear poly-amino-saccharides resulted from the N-deacetylation of chitin. The latter is the second most abundant natural polymer on the biosphere after cellulose. Chitin deacetylation is a non-enzymatic process in which R-NHCOCH₃ residue is removing and treating with strong alkali at high temperatures. Chitosan become soluble in acidic aqueous solutions when the degree of deacetylation become higher than 50% resulting in a protonation of amine groups in the presence of H⁺ ions that makes the chitosan behaves as a cationic polyelectrolyte [1, 2]. Chitosan possesses enormous properties and unique features being a biodegradable, biocompatible, renewable, non-cytotoxic and efficient against bacteria, viruses and fungi [3-5]. Chitosan was used in agriculture to control the release time of fertilizers into soils, in waste water treatment, as a preservative in food and beverages, in cosmetics to maintain skin moisture and treat acne, in biopharmaceutics and, as antibacterial agent [6, 7]. The antibacterial activity of chitosan is due to its ionic interaction on the surface and inside the bacterial cells. The positive charges of chitosan-based materials ionize the negatively charged molecules settled on the bacterial cells` surface. In addition, chitosan penetrates inside the bacterial cells and inhibit the proteins synthesis by interacting with the negatively charged mRNA blocking its further processing inside the cell [8]. Chitosan can be easily processed in distinct forms, including films, microparticles, nanofibers and nanoparticles [9, 10]. These forms have been used for various applications.

Chitosan based nanoparticles (CSNPs) showed great interest as polymeric drug delivery system. CSNPs have superior advantages in nanomedicine with improved bioavailability when compared with traditional drug carrier systems. CSNPs are available in many sizes and shapes with increased specificity and sensitivity [11, 12]. The rising occurrence of antibacterial resistance of many antibiotics due to their overuse threatened their

ability to treat a huge number of diseases and infections. Accordingly, researchers were directed recently to the use of nanoparticles to overcome resistance.

Ciprofloxacin is an antibiotic from the quinolone family. Quinolones are one of the most commonly used and prescribed antibiotics to treat urinary tract, skin, intraabdominal and pelvic infections as well as sexually transmitted diseases and chronic bronchitis [13-16]. As mentioned earlier that antibiotic resistance is threatening the use of drugs. Quinolones resistance mechanisms are grouped into three discrete categories: target mediated, plasmid mediated and chromosome mediated quinolone resistance. The cellular alterations associated with each mechanism can accumulate creating strains with very high levels of quinolones resistance [13].

In this work ciprofloxacin HCl was loaded in chitosan-based nanoparticles from insects and crustacean sources from Egypt to overcome the bacterial resistance mechanisms using both gram-positive and gram-negative bacteria. The minimum inhibitory concentration was examined. In addition, a complete release profile for ciprofloxacin HCl was performed and explained.

2. Experimental procedures:

2.1. Materials

Chitosan obtained from desert locust (*Schistocerca gregaria*) reared in the Entomology Department, Faculty of Sciences, Cairo University, beetles (*Calosoma rugosa*) and honey bee (*Apis mellifera*) exoskeletons collected from Giza governorates and shrimp (*Peanous mondon*) shells purchased from local Egyptian market. Trisodium polyphosphate, acetic acid, HCl, and NaOH purchased from Sigma Chemical Co. USA. Ciprofloxacin-HCl acquired from Bio World USA. *Escherichia coli* (ATCC = 25922), *Bacillus thuringiensis* (ATCC = 6633) and Methicillin-resistant *Staphylococcus aureus* MRSA (ATCC = 6538), and *Pseudomonas aeruginosa* (ATCC = 7853) provided by the Microbiology Centre, Faculty of

Agriculture, Ain Shams University, Cairo, Egypt. Muller Hinton broth was purchased from Oxoid, UK.

2.2. Method:

2.2.1. Preparation of chitosan:

Chitin isolated from desert locust (*Schistocerca gregaria*), beetles (*Calosoma rugosa*) and honey bee (*Apis mellifera*) exoskeletons and shrimp (*Penaeus monodon*) shells following the standard procedures as described before [17]. Briefly, the exoskeleton of insects as well as shrimp shells were soaked and boiled in 1N NaOH for deproteinization till obtaining a clear solution. The resulted solid fraction was then treated with 36.5% HCl solution at ambient temperature with a solution to solid ratio 15 ml/g for demineralization. The purified chitin was dried in vacuum oven at 50 °C to constant weight [17-20]. The chitin was then deacetylated to chitosan by drenching into 50% NaOH at 100 °C for 8 hrs. The resulted chitosans from shrimp (SCS), locust (LCS), beetles (BCS) and honey bee (HCS) were dried in vacuum oven at 50 °C for 24 hrs.

2.2.2. Characterization of chitosan

2.2.2.1. Fourier transform infrared spectroscopy (FTIR)

FTIR spectra of SCS, LCS, BCS and HCS were recorded after deacetylation using the Nicolet iSTM10 FTIR Spectrometer, Thermo Fisher Scientific USA. Specimens were placed on the KBr diamond. The spectral region between 4000 and 400 cm^{-1} was scanned with a resolution of 2 cm^{-1} within 20 scans.

2.2.2.2. X-ray diffraction (XRD):

XRD analysis was used to evaluate their crystallinity, and their diffraction patterns were recorded by PANalytical X'Pert PRO X-ray machine (Netherland). The X-ray source was Cu $K\alpha$ radiation (45 kV, 30 mA). Samples were scanned from $2\theta = 5-40^\circ$ at a scanning

rate of 4 min^{-1} and a measuring temperature of $25 \text{ }^\circ\text{C}$ [21]. The percentage of the polymer crystallinity was determined from equation (1):

$$\text{Crystallinity \%} = [(I_{110} - I_{\text{amp}}) / I_{110}] \times 100 \quad (1)$$

Where, I_{110} is the intensity at $2\theta \approx 16^\circ$ and I_{amp} is the amorphous intensity.

2.2.2.3. Determination of the degree of deacetylation (DD) of CS:

The degree of deacetylation (DD) of chitosan was measured by using titration method. Separately, 0.5 g of chitosans were weighted, and dissolved in 20 mL 0.3N HCl at room temperature then the volume was completed to 400 ml using distilled H_2O . Chitosans solutions were titrated against 1N NaOH solution in the presence of a pH meter (Thermoscientific, USA). A titration curve of pH vs. NaOH titration volume was generated. The curve's inflection points were found for each indicated transition. The volume of NaOH at each inflection point was applied to equation (2):

$$\text{DD\%} = 16.1(y-x)/W \quad (2)$$

Where W is the weight of chitosan, x is the first inflection point on the graph of measured pH vs. titration volume, and y is the second inflection point [17, 22].

2.2.3. Preparation of chitosan nanoparticles and ciprofloxacin loaded nanoparticles:

Chitosan nanoparticles (CSNPs) were prepared by ionic crosslinking of chitosan with trisodium polyphosphate (TPP) from the four chitosan sources as described previously. Briefly 0.033 mg/ml TPP were added dropwisely during homogenization to 0.2 g. CS dissolved in 1% acetic acid. Each sample was homogenized for 30, 60, 90, and 120 min. using the PT-3100 Polytron at 10000 rpm, Kinematics, Switzerland homogenizer. For ciprofloxacin loaded nanoparticles, 1 g. of ciprofloxacin HCl was dissolved in the chitosan solution before adding TPP. This preparation was done by using strongly acidic chitosan pH = 3.5- and 30-min homogenization at 10000 rpm only. Each CSNPs group was prepared and analyzed in triplicates [23]. The prepared CS based nanoparticles from SCS, LCS, BCS and

HCS were signified as SCSNPs, LCSNPs, BCSNPs and HCSNPs, respectively. The ciprofloxacin loaded CSNPs prepared from SCS, LCS, BCS and HCS were signified as Cipro-SCSNPs, Cipro-LCSNPs, Cipro-BCSNPs and Cipro-HCSNPs, respectively.

2.2.4. Chitosan nanoparticles characterization:

Particle size distribution and Zeta potential (ZP) of SCSNPs LCSNPs, BCSNPs and HCSNPs were determined by photon correlation spectroscopy and laser Doppler anemometry, respectively using Zetasizer Nano ZS 3500 (Malvern instrument). Samples were diluted with 0.1 KCl and placed in an electrophoretic cell where a potential of ± 150 mV was established. The calculations of the ZP with Smoluchowski's equation from the mean electrophoretic mobility value were studied. Each sample was analysed in triplicate [23, 24].

2.2.5. Encapsulation efficiency:

The amount of ciprofloxacin encapsulated by Cipro-SCSNPs, Cipro-LCSNPs, Cipro-BCSNPs and Cipro-HCSNPs prepared was determined by centrifugation method. The redispersed nanoparticles suspension was centrifuged at 10000 rpm for 1 hour at 15 °C. The supernatant was taken to measure the free drug content by using UV-visible spectrophotometer (UV-1002M201; 5000 Carry Varian; Agilent; US) at 272 nm after suitable dilution. The Drug entrapment efficiency (%EE) was calculated from equation (3):

$$EE\% = (\text{Experimental drug content}/\text{Theoretical drug content}) \times 100 \quad (3)$$

Samples were prepared and analysed in triplicates [25].

2.2.6. In vitro release profile:

The release profile of Ciprofloxacin HCl from Cipro-SCSNPs, Cipro-LCSNPs, Cipro-BCSNPs and Cipro-HCSNPs was checked after 10 hours incubation in water at 37 °C as described previously [25-27]. Briefly, dialysis tubes were used with an artificial membrane (SERVA visking® with 16 nm tubing diameter). The prepared CSNPs loaded with

ciprofloxacin were redispersed in 5 ml PBS (phosphate buffer saline) pH = 7.4. The dialysis tubes were then immersed in a container containing 100 ml PBS with continuous stirring and a sample was taken every 1 hour to measure the amount of ciprofloxacin released from the membranes using UV-visible spectrophotometer (UV-1002M201; 5000 Carry Varian; Agilent; US) at 272 nm.

2.2.7. Drug release data analysis (model fitting kinetics):

The results of the kinetic and mechanism of the *in vitro* release of ciprofloxacin were fitted with a series of kinetic equations to understand the drug release kinetic mechanism. These equations include zero order, first order, Higuchi and Korsmeyer Peppas model. Zero order model where the drug is released slowly from the dosage form and does not aggregate. This model describes the release rate which is concentration independent. It is represented by the relation between the cumulative release percent vs. time. It is expressed by equation (4):

$$Q_t = Q_0 + K_0t \quad (4)$$

Where Q_t is the amount of drug dissolved in time t , Q_0 is the initial amount of drug in the solution and K_0 is the zero order release constant. First order model is a system where the release rate is concentration dependent. It has been used to study the absorption or elimination of some drugs. It is described by the relation between log % of the remaining drug vs. time t and it is expressed by equation (5):

$$\text{Log } Q_t = \text{Log } Q_0 + (K_1t/2.303) \quad (5)$$

Where Q_t is the amount of drug dissolved in time t , Q_0 is the initial amount of drug in the solution and K_1 is the first order release constant. Higuchi model refers to a release system in which the drug is released from insoluble matrix as a square root of time process and it depends on Fickian diffusion. Higuchi model is the relation between the cumulative drug release percent vs. square root of time. It is expressed by equation (6):

$$Q_t = K_Ht^{1/2} \quad (6)$$

Where K_H is the Higuchi dissolution constant. Korsmeyer- Peppas model which is the relation between the log of cumulative % of drug release vs. log the time and it is expressed by equation (7):

$$Q_t/Q_\infty = K_k t^n \quad (7)$$

Where K_k is the Korsmeyer constant, n is the release exponent and Q_t/Q_∞ is the function of t . The R^2 which is the coefficient of correlation is obtained from the four described equations. It is known that the Korsmeyer Peppas model is widely used to determine the diffusion mechanism according to the exponent value (n) (Table 1) [26-33].

Release exponent (n)	Drug transport mechanism
$n < 0.5$	Fickian diffusion
$0.5 < n < 1$	Anomalous transport
$n = 1$	Case II transport
$n > 1$	Super case II transport

Table 1: interpretation of release diffusion mechanisms

2.2.8. Antibacterial activity testing of CSNPs:

Minimal inhibitory concentrations (MIC) were determined as the lowest concentrations of SCS, LCS, BCS, HCS, SCSNPs LCSNPs, BCSNPs, HCSNPs as well as Cipro-SCSNPs, Cipro-LCSNPs, Cipro-BCSNPs and Cipro-HCSNPs at which microorganisms cannot grow in Müller Hinton broth based on the method of Ruparelia *et al.* [34]. The MIC was tested on two-gram negative bacteria (*Escherichia coli* (ATCC = 25922), *Bacillus thuringiensis* (ATCC = 6633)) and two-gram positive bacteria (Methicillin-resistant *Staphylococcus aureus* MRSA (ATCC = 6538), and *Pseudomonas aeruginosa* (ATCC = 7853)) and was determined by microdilution broth technique using Mueller-Hinton medium [35]. Briefly, 50 μ l from each sample to be tested was serially diluted 12 folds in a 96 well

plate then a 100 μl of the Müller Hinton broth were added on every well followed by 50 μl from the tested bacterial species. The samples were incubated for 24 hrs. The absorbance values were then measured and plotted.

2.2.9. Statistical analysis:

Results were presented as average arithmetic mean and error bars represent \pm standard deviation (SD). For all experiment average values were reported from three independently prepared samples. Results were evaluated statistically by the Statistical Package for Social Sciences (SPSS), using independent T test, and one-way ANOVA test with considering a p-value of less than and equal to 0.05 significant.

3. Results and discussion:

3.1. Physicochemical characterization of CS:

3.1.1. Fourier transform infrared spectroscopy (FTIR)

The chemical structure of the chitosans derived from the tested species is confirmed by FTIR analysis [Figure.1]. As seen, the absorption peaks that appear as a doublet overlapped bands at around 1663 and 1618 cm^{-1} are corresponding to amide I (due to $-\text{C}=\text{O}$ stretching of hydrogen bonded $-\text{C}=\text{O}-\text{NHCH}_3$ group), indicating that the isolated chitosans from the 4 tested species (SCS, LCS, HCB and BCS) are in the α -form [36-41]. The amide II (due to N-H bending of NH_2 group) bands appear at round 1589 cm^{-1} [36-41]. For the SCS, these peaks appeared at 1650 and 1586 cm^{-1} , respectively. The absorption band at 3000–3500 cm^{-1} is due to symmetric stretching vibration of NH_2 and OH groups. The C-H stretching absorption peak appears at around 2885 cm^{-1} . The N-H bending vibration of primary amides and C-O-C stretching absorption peaks appears at 1326 and 1080 cm^{-1} , respectively [42, 43].

3.1.2. X ray diffraction (XRD):

XRD patterns of the obtained four species chitosans are shown in [Figure.2]. SCS exhibited two sharp diffraction peaks at 9.4° and $20.2^\circ\theta$. LCS showed three sharp peaks at

9.3°, 20.2° and 24.4°θ. For HCS, two intense main peaks at 9.7° and 20.3°θ were observed. For BCS, two strong peaks at 9.7°, and 20.3°θ were examined. All examined peaks were like those observed in chitosan structures obtained from different organisms such as insects, crustaceans, anthozoans and fungi [44-51]. The two sharp peaks characterize chitosan appeared at around 10° and 20° θ that corresponding to the (0 2 0) and (1 1 0) planes of the crystalline [52, 53]. The estimated crystallinity index (CI %) was found to be 69, 61, 59 and 49%, for LCS, SCS, HCS and BCS chitosan, respectively. This indicates that the LCS and BCS were the highest and the lowest crystallinity, respectively, compared to the other species studied.

3.1.3. Degree of deacetylation (DD):

The most important parameter that influences chitosan various properties including physicochemical, biological, and mechanical properties is its degree of deacetylation (DD). It depends on the method of isolation. Therefore, the reaction conditions should be taken into consideration prior to the use of chitosan as drug delivery system [54]. One-way ANOVA was used to study the statistical significance between the samples where $P \leq 0.05$ is considered significant. The results were expressed as average arithmetic means, and error bars represent \pm SD. Results revealed that the relation between LCS to SCS, SCS to BCS, and SCS to HCS were significant. Our results showed that the DD of LCS was the highest 98% followed by HCS 96% and from BCS 95%, while SCS had the lowest DD 74% [Figure.3].

3.2. Chitosan nanoparticles (CSNPs) characterization:

3.2.1. Particle size distribution and Zeta Potential (ZP):

Different techniques have been used to determine nanoparticles size. These include, scanning electron microscope (SEM), transmission electron microscope (TEM), and the dynamic light scattering (DLS). DLS measure the mean particle size distribution as well as ZP of the nanoparticles. SEM, and TEM can give prominent understanding about the particle

size and morphology [55], but DLS can be used to find the NPs size at extremely low level. The nanoparticles were formed spontaneously under homogenization upon the incorporation of the prepared tri-sodium polyphosphate (TPP) solution to the chitosan solution. CSNPs were obtained by the ionotropic gelation method which is a simple process, where particles are formed by means of electrostatic interactions between the positively charged CS chains and the polyanions of the TPP. The effect of homogenization time during the preparation of CSNPs was evaluated. Statistical significance between samples at each time point was evaluated using one-way ANOVA where $P \leq 0.05$ significant, and $P > 0.05$ non-significant. The results were expressed as average arithmetic means. Error bars represents \pm SD. The results showed that at 30 min homogenization the SCSNPs relations to LCSNPs and BCSNPs were significant [Figure 4 (A)], while at 60 min, all the relations were non-significant [Figure 4 (B)]. For the 90 min homogenization, it was found that the relations SCSNPs to BCSNPs, LCSNPs to BCSNPs, and HCSNPs to BCSNPs were significant [Figure 4 (C)]. Finally, at 120 min, all the relations were significant except SCSNPs to LCSNPs and HCSNPs.

A general trend showed an increase in the mean particle size distribution of nanoparticles with the increase of homogenization time from 30 to 120 min in all sources except in SCSNPs, the size decreased at 120 min. The mean particle size distribution increased significantly only in LCSNPs and BCSNPs from 36.7 ± 3.59 nm to 125.9 ± 18.24 nm, and from 55.48 ± 10.34 nm to 408.9 ± 39.75 nm, respectively. This is explained by crosslinking of more TPP with the CS molecules, leading to an increase in the mean particle size. The mean particle size at 30 min homogenization of LCNPs was the smallest followed by HCNPs, BCNPs, and SCNPs, respectively [Figure 4 (A)]. Their mean size distribution ranged from 36.7 ± 3.59 nm to 114.36 ± 53.51 nm. At 60 min homogenization, the smallest mean particle size was of the HCSNPs followed by LCNPs, BCNPs, and SCNPs, respectively [Figure 4 (B)]. Their mean size distribution ranged from 74.42 ± 4.29 nm to 183.9 ± 30.38

nm. At 90- and 120-min homogenization, the mean particle size of LCNPs was the smallest followed by SCNPs, HCNPs, and BCNPs, respectively [Figure 4 (C & D)].

ZP analysis by the DLS is an important technique used to determine the surface charge and predicting the long-term stability of nanoparticles in solution. The stability behaviour of the nanoparticles is based on the ZP results itself as a number no matter this number is positive or negative. The results behaviour relation of ZP was classified into 5 groups: from 0 to ± 5 mV rapid coagulation, from ± 10 to ± 30 mV incipient stability, from ± 30 to ± 40 mV moderate stability, from ± 40 to ± 60 mV good stability, and more than ± 61 mV excellent stability [56]. ZP is a crucial parameter for stability in aqueous nanosuspensions, a ZP of at least ± 30 mV is required as a minimum for nanoparticles stability [57]. One-way ANOVA was used to study the statistical significance between nanoparticles ZP at the different time points where $P \leq 0.05$ is significant, and $P > 0.05$ is non-significant. Results were expressed as average arithmetic mean, and error bars represent \pm SD. Results showed that at 30 min the significance was the highest, while at 60, and 120 min only the relation between SCSNPs and BCSNPs was significant. However, at 90 min, all the relations were non-significant [Figure 5]. The ZP of CSNPs had its highest values at 30 min homogenization. The highest was HCSNPs followed by SCSNPs, BCSNPs, and LCSNPs, respectively. It ranges from excellent to good stability [56], 62.5 ± 4.01 mV to 42.27 ± 1.31 mV, respectively [Figure 5 (A)]. Moreover, at 60 and 90 min, the values were in the following orders: the highest was SCSNPs followed by HCSNPs, LCSNPs, and BCSNPs, respectively [Figure 5 (B & C)]. It ranges from 54.5 ± 1.39 mV to 43.45 ± 7.68 mV, and from 54.30 ± 2.44 mV to 46.70 ± 5.36 mV in 60 min, and 90 min, respectively, indicating a good stability. Finally, at 120 min, the highest was also SCSNPs followed by LCSNPs, HCSNPs, and BCSNPs, respectively [Figure 5 (D)]. It ranges from 54.83 ± 0.66 mV to 43.07 ± 7.35

with good stability. According to the obtained results, the preparation of the ciprofloxacin loaded nanoparticles was done under 30 min homogenization only.

3.3. Particle size, zeta potential of Ciprofloxacin loaded CSNPs:

Mean particle size distribution and ZP are necessary characteristic parameters for nanosuspensions formulations [57]. CS and TPP concentration, and stirring speed were affecting factors on the mean particle size distribution. Particle size reduction less than 1 μm is improving solubility of drugs and can be used as a drug delivery system. Although, reduction of particle size below 1 μm improve drugs` solubility, technologies have reduced the particle size to the nm size range [58]. This has been reached in this study. The largest particle size used was 114.36 ± 53.51 nm and 267.50 ± 4.99 nm before loading drug, and after loading drugs, respectively, for the SCSNPs. In addition, statistical significance study using paired t-test within the same type of nanoparticles before and after loading ciprofloxacin, where $P \leq 0.05$ was considered significant. Results showed that in the particles size all the relations were significant except in the HCSNPs group. In the ZP, the relations in LCSNPs, and BCSNPs were significant. In the present study, the ciprofloxacin loaded CSNPs preparation from SCS, LCS, HCS, and BCS was performed under 30 min homogenization at 10000 rpm. The transformation of CS solution from clear to turbid is an indication that the solution became at the nanoscale due to the incorporation of CS/TPP [59]. Increasing the amount of drug in drug polymer ratios was found to increase slightly the average drug entrapment efficiency of the nanoparticles` formulations [60]. In the present study, the drug entrapment efficiency of nanoparticles containing 1000 mg ciprofloxacin was almost the same 99.8% for HCSNPs followed by 99.7% for SCSNPs, and 99.4% for both LCSNPs and BCSNPs as measured from remaining drug content in the supernatant after the loading process. This high entrapment efficiency is due to the electrostatic interactions between the ciprofloxacin and CS. In a similar study, the average entrapment efficiency was

decreased by increasing the amount of drug in the polymer drug ratio, this may be due to the saturation capacity of nanoparticles [60]. The particle size measurements before drug loading (BDL), and after drug loading (ADL) reflected the interaction between the drug and the polymer. CSNPs has mean particle size distribution ranged from 36.71 ± 3.59 nm to 114.36 ± 53.51 nm from the four sources used in this study, where LCSNPs had the lowest particle size while the SCSNPs had the highest particle size [Figure 4 (A)] and [Figure 6 (A)]. It was found that the particle size increased from 36.71 ± 3.59 nm to 91.38 ± 0.56 nm in LCSNPs, from 51.59 ± 8.48 nm to 70.54 ± 0.91 nm in HCSNPs, from 55.48 ± 10.34 to 91.67 ± 0.65 in BCSNPs, and from 114.36 ± 53.51 nm to 267.50 ± 6.12 nm in SCSNPs when ciprofloxacin was added [Figure 6 (A)]. Similar results were obtained by Srinatha et al who reported that chitosan beads size increased markedly with an increase in ciprofloxacin drug loading [61]. The ZP of CSNPs from the four sources ranged from 62.5 ± 4.01 mV to 42.27 ± 1.31 mV under the effect of 30 min homogenization before adding ciprofloxacin [Figure 5 & 6 (A)]. Similar results were obtained in pervious study [62]. The ZP of SCSNPs and HCSNPs was almost the same BDL and ADL, from 55.20 ± 1.63 mV to 55.23 ± 0.06 mV and from 62.50 ± 4.01 mV to 62.53 ± 0.55 mV, respectively. In BCSNPs, ZP decreased from 45.60 ± 6.10 mV to 42.27 ± 5.86 mV, while in LCSNPs, ZP increased from 42.27 ± 1.31 mV to 55.87 ± 1.07 mV [Figure 6 (B)]. This may be due to the positive charge carried by the ciprofloxacin loaded onto CSNPs. These results agreed with the results obtained by Du *et al.* in 2009 who reported that the ZP of CSNPs were increased when metal ions were loaded [62]. All these data and results obtained indicate that ciprofloxacin loaded CS based nanoparticles prepared in this study followed all the criteria of a highly stable drug delivery system.

3.4. In vitro release profile of ciprofloxacin from CSNPs and kinetic modelling:

The kind of drug, crystallinity particle size, and its polymorphic form affect the release kinetic. The kinetic models are used to describe the drug dissolution mechanism from

the prepared formulations [63]. The release of water-soluble drug incorporated in a matrix is mainly by the aid of diffusion as in the case of the ciprofloxacin used, while in the low water-soluble drugs the release is by self-erosion from the matrix [64]. The formulations of Cipro-SCSNPs, Cipro-LCSNPs, Cipro-BCSNPs and Cipro-HCSNPs were subjected to *in vitro* dissolution studies in phosphate buffer saline pH =7.2 showing a sustained drug release mechanism which is very important in many fields of applications. The release profile of Cipro/SCSNPs, Cipro/LCSNPs, Cipro/BCSNPs and Cipro/HCSNPs [Figure 7], showed an initial gradual release of the drug, and then reaching a plateau. The maximum amount of drug was released during the 6th, 7th, 6th and the 4th hour from Cipro-SCSNPs, Cipro-LCSNPs, Cipro-HCSNPs and Cipro-BCSNPs, respectively. The amount of the drug release was 72.62%, 94.68%, 53.68% and 93.82% for Cipro-SCSNPs, Cipro-LCSNPs, Cipro-HCSNPs and Cipro-BCSNPs, respectively. These results were explained by using four of the most common kinetic profiles used: zero order, first order, Higuchi and Korsmeyer Peppas model. Sirinatha, et al used first order and Higuchi model to analyse the release kinetics of ciprofloxacin from chitosan. They reported that the loading of different chitosan/ciprofloxacin ratios affects the amount of drug released and its kinetic in physiological solutions. Additionally, higher ciprofloxacin chitosan ratios increased the ciprofloxacin release [61].

The release kinetics modelling data of the Cipro-SCSNPs, Cipro-LCSNPs, Cipro-BCSNPs and Cipro-HCSNPs formulations have been indicated in Table 2. The zero-order kinetics is used to describe the release of drugs in case of some transdermal systems, osmotic systems and coated forms. The formulations following this profile release the same amount of drug by unit of time which is not the case of any of our formulations as it is used to achieve release for prolonged action [65]. The formulations of water-soluble drugs in porous matrices follow the first order kinetic release profile; it releases the drug in a way that is proportional

to the amount of the remaining drug in the interior of the formulation. In such a way the amount of drug released is decreased by unit of time [66]. According to the higher value of regression coefficient both Cipro-LCSNPs and Cipro-HCSNPs formulations followed the first order release kinetics showing the effect of the porous and fibrous structure as previewed in their SEM micrographs of CS obtained from locust and honey bee [17]. The Higuchi model was used to study the release of water soluble and soluble drugs which was incorporated into semi-solid or solid matrixes which was not the case in any of the prepared formulations [67]. The Korsmeyer Peppas model have been used to describe the release of polymeric dosage forms when the release mechanism was not well known or when more than one type of release could be involved [68]. The Cipro-SCSNPs and Cipro-BCSNPs formulations followed the Korsmeyer Peppas model kinetics indicating that they are polymeric porous systems which is reflected in their surface morphology [Figure 2 (B and C)]. The higher values of regression coefficient were found to be 0.955, 0.9972, 0.9476 and 0.9602 for Cipro-SCSNPs, Cipro-LCSNPs, Cipro-BCSNPs and Cipro-HCSNPs, respectively. Moreover, the n values for Korsmeyer Peppas model were 0.498, 0.524, 0.598 and 0.385 for Cipro-SCSNPs, Cipro-LCSNPs, Cipro-HCSNPs and Cipro-BCSNPs, respectively, indicating Fickian release for Cipro-SCSNPs and Cipro-HCSNPs, and non- Fickian release for Cipro-LCSNPs and Cipro-BCSNPs [69].

Formulation	Zero Order Kinetics	First Order Kinetics	Higuchi Model	Korsmeyer-Peppas Model		Type of Transport
	Regression Coefficient (R^2)				N	
Cipro/SCSNPs	0.4436	0.8809	0.9504	0.9550	0.498	Fickian diffusion
Cipro/LCSNPs	0.5442	0.9972	0.9600	0.9617	0.524	Non- Fickian diffusion
Cipro/HCSNPs	0.2610	0.9476	0.8809	0.9441	0.385	Fickian diffusion
Cipro/BCSNPs	0.7242	0.9175	0.9400	0.9602	0.598	Non-Fickian diffusion

Table 2: Mathematical Model used to describe the drug release

3.5. In Vitro testing of antimicrobial activity:

CS was known by its biological activity including antitumor, wound healing and antimicrobial activity. The antibacterial activity of CS has been widely explored due to the absence of bacterial resistance to CS [70]. CS exhibit broad spectrum of inhibition against both Gram positive and Gram-negative bacteria [71]. The antibacterial activity of ciprofloxacin loaded CSNPs from different CS sources have been assessed against four different bacterial strains by determining the minimum inhibitory concentration (MIC) values [Table 3]. Gram positive strains statistical significance difference between groups within the same strain was shown in [Figure 8], while gram negative strains in [Figure 9]. Error bars represents \pm SD. One-way ANOVA was used, and statistical analysis significance was observed ($P \leq 0.05$ significant, and $P > 0.05$ non-significant). In *P. aeruginosa*, and MRSA all the ciprofloxacin loaded nanoparticles were statistically significant. In *E. coli* and *B. thuringiensis* most of the samples were statistically significant. The non-significant relations were visualised in [Figure 8 & 9]. The antibacterial activity of CSNPs and ciprofloxacin loaded CS based nanoparticles (Cipro/CSNPs) were compared with that of CS prepared from different sources and ciprofloxacin alone. The ciprofloxacin MIC values vary according to the bacterial strain. It has been showed that the highest antibacterial activity was against *E. coli* while, it showed the lowest antibacterial activity against *P. aeruginosa*. On the other hand, the Cipro/CSNPs from the four different sources (locust, honey bee, beetles and shrimp) showed the highest antibacterial activity against *E. coli* and MRSA with MIC varies from 0.0043 to 0.01 $\mu\text{g/ml}$ and from 0.07 to 0.14 $\mu\text{g/ml}$, respectively. Enhancing the efficacy of antibacterial agents loaded into polymeric nanoparticles is reported in numerous studies [72-74]. SCS and SCSNPs showed antibacterial activity against *B. thuringiensis* with the same MIC value of 1.09 $\mu\text{g/ml}$. The unloaded LCSNPs and Cipro/LCSNPs inhibited the

growth of *E. coli* with MIC values of 2.17 and 0.0043 $\mu\text{g/ml}$, respectively. Meanwhile, the MIC of ciprofloxacin was 0.03 $\mu\text{g/ml}$ against the same microorganism. This means that the inhibitory effect of ciprofloxacin was enhanced by its entrapment by LCSNPs. The same results were observed in Cipro/SCSNPs, Cipro/BCSNPs, Cipro/HCSNPs except that ciprofloxacin and Cipro/HCSNPs showed the same antibacterial activity against MRSA with MIC of 0.14 $\mu\text{g/ml}$. LCSNPs obtained in the present study had small particle size, which may increase the drug penetration into the bacterial cell and improve its antibacterial activity compared with the nanoparticles prepared from the other 3 sources. Sobhani et al reported that the MIC values were decreased significantly by 50 % when charged with ciprofloxacin loaded HCl loaded CS nanoparticles for *E. coli* and *S. aureus* [75]. In a similar study, the chitosan/protamine nanoparticles increased the antibacterial activity of chitosan nanoparticles against *E. coli* [75]. In similar studies, when chitosan was loaded with metals, it have been reported that silver loaded CS nanoparticles showed the highest antibacterial activity against *E.coli* and *Staphylococcus aureus* with MIC of 3 and 6 $\mu\text{g/ml}$, respectively [61], and CS loaded with Cu^{2+} inhibited the bacterial growth of various microorganisms and exhibited higher antibacterial activity than that of CS solution or the doxycycline which was used as positive control [76]. In addition, an enhanced antibacterial activity of ciprofloxacin loaded ZnO nanoparticles against *staphylococcus aureus* and *E coli* was also reported. We explained that by the direct nanoparticles' interference with N or A protein pumping activity of the tested bacterial strains [77]. According to our data, the antibacterial activity of CSNPs, and Cipro/CSNPs are significantly higher than that of CS and free drug itself. Moreover, the MIC value of ciprofloxacin against the four different bacterial strains are lower than those of CSNPs, which indicate higher antibacterial activity. Antibacterial activity is also inversely affected by the pH, with higher activity observed at lower pH values. This explained the higher antibacterial activity of our samples prepared at acidic pH (3.5) [78].

Sample	Gram negative strains		Gram positive strains	
	<i>B. thuringiensis</i>	<i>E.coli</i>	MRSA	<i>P. aeruginosa</i>
	MIC concentration $\mu\text{g/ml}$			
CiproSCSNPs	0.07	0.01	0.07	0.27
CiproLCSNPs	0.03	0.0043	0.07	0.54
CiproHCSNPs	0.03	0.008	0.14	1.09
CiproBCSNPs	0.03	0.0084	0.03	1.09
SCSNPs	1.09	1.09	2.17	2.17
LCSNPs	2.17	2.17	2.17	2.17
HCSNPs	1.09	1.09	1.09	2.17
BCSNPs	0.27	2.17	2.17	2.17
SCS	1.09	2.17	1.09	2.17
LCS	2.17	2.17	2.17	2.17
HCS	2.17	2.17	2.17	2.17
BCS	2.17	2.17	2.17	1.09
Ciprofloxacin	0.14	0.03	0.14	2.17

Table 3: MIC Concentration/ μg of chitosan sample from different sources

4. Conclusion:

In summary, ciprofloxacin chitosan-based nanoparticles (Cipro/CSNPs) from different CS sources have been prepared and characterized in the present study. Chitosan nanoparticles (CSNPs) enhanced drug delivery, allowed its controlled release as well as enhancing its antibacterial activity. The locust chitosan-based nanoparticles (LCSNPs) obtained in the present study had the smallest particle size $36.7 \text{ nm} \pm 3.59$ which increased the drug penetration into the *Escherichia coli* bacterial cell and improve its antibacterial

activity after drug loading compared with the nanoparticles prepared from the other 3 sources. MIC value was 85.6% lower than the MIC of the free drug itself. The results showed that Cipro/CSNPs could inhibit the growth of four types of gram positive and negative bacteria markedly and showed higher antibacterial activity than CSNPs or CS solution itself. It was predicted that CSNPs could be used in medicine as a carrier for antimicrobial agents for their antibacterial activity and their biocompatibilities.

ACCEPTED MANUSCRIPT

5. References:

- [1] I. Younes, O. Ghorbel-Bellaaj, M. Chaabouni, M. Rinaudo, F. Souard, C. Vanhaverbeke, K. Jellouli, M. Nasri, Use of a fractional factorial design to study the effects of experimental factors on the chitin deacetylation, *Int. J. Biol. Macromol.* 70 (2014) 385-390.
- [2] T.C.M. Stamford, T.M. Stamford-Arnaud, H.M.d.M. Cavalcante, R.O. Macedo, G.M.d. Campos-Takaki, Microbiological Chitosan: Potential Application as Anticariogenic Agent, in: A.O. Andrade, A.A. Pereira, E.L.M. Naves, A.B. Soares (Eds.), *Practical Applications in Biomedical Engineering*, InTech, Rijeka, 2013, p. Ch. 09.
- [3] P.K. Dutta, J. Dutta, V. Tripathi, Chitin and chitosan: Chemistry, properties and applications, *J. Scien. Ind. Res.* 63 (2004) 20-31.
- [4] E.I. Rabea, M.E.-T. Badawy, C.V. Stevens, G. Smagghe, W. Steurbaut, Chitosan as antimicrobial agent: applications and mode of action, *Biomacromol.* 4 (2003) 1457-1465.
- [5] N. Angelova, N. Manolova, I. Rashkov, V. Maximova, S. Bogdanova, A. Domard, Preparation and properties of modified chitosan films for drug release, *J. bioact. Compat. Pol.* 10 (1995) 285-298.
- [6] M. Rinaudo, Chitin and chitosan: Properties and applications, *Prog. Polym. Sci.* 31 (2006) 603-632.
- [7] M.N.V.R. Kumar, R.A.A. Muzzarelli, C. Muzzarelli, H. Sashiwa, A.J. Domb, Chitosan Chemistry and Pharmaceutical Perspectives, *Chem. Rev.* 104 (2004) 6017-6084.
- [8] A. MATICA, G. MENGHIU, V. OSTAFE, ANTIBACTERIAL PROPERTIES OF CHITIN AND CHITOSANS, *New Front. Chem* 26 (2017) 39-54.
- [9] J.Y. Kim, J.K. Lee, T.S. Lee, W.H. Park, Synthesis of chitooligosaccharide derivative with quaternary ammonium group and its antimicrobial activity against *Streptococcus mutans*, *Int. J. Biol. Macromol.* 32 (2003) 23-27.

- [10] C.E. Orrego, N. Salgado, J.S. Valencia, G.I. Giraldo, O.H. Giraldo, C.A. Cardona, Novel chitosan membranes as support for lipases immobilization: Characterization aspects, *Carbohydr. Polym.* 79 (2010) 9-16.
- [11] X. Li, J. Gao, Y. Yang, H. Fang, Y. Han, X. Wang, W. Ge, Nanomaterials in the application of tumor vaccines: advantages and disadvantages, *Onco Targets ther.* 6 (2013) 629-634.
- [12] A. Ghadi, S. Mahjoub, F. Tabandeh, F. Talebnia, Synthesis and optimization of chitosan nanoparticles: Potential applications in nanomedicine and biomedical engineering, *Caspian J. inter. Med.* 5 (2014) 156-161.
- [13] K.J. Aldred, R.J. Kerns, N. Osheroff, Mechanism of quinolone action and resistance, *Biochem.* 53 (2014) 1565-1574.
- [14] V.T. Andriole, The quinolones: past, present, and future, *Clin. Infect. Dis.* 41 (2005) 113-119.
- [15] K. Drlica, H. Hiasa, R. Kerns, M. Malik, A. Mustaev, X. Zhao, Quinolones: action and resistance updated, *Current top. Med. Chem.* 9 (2009) 981-998.
- [16] A. Dalhoff, Resistance surveillance studies: a multifaceted problem—the fluoroquinolone example, *Infect.* 40 (2012) 239-262.
- [17] N.H. Marei, E.A. El-Samie, T. Salah, G.R. Saad, A.H.M. Elwahy, Isolation and characterization of chitosan from different local insects in Egypt, *Int. J. Biol. Macromol.* 82 (2016) 871-877.
- [18] R.H. Rødde, A. Einbu, K.M. Vårum, A seasonal study of the chemical composition and chitin quality of shrimp shells obtained from northern shrimp (*Pandalus borealis*), *Carbohydr. Polym.* 71 (2008) 388-393.
- [19] E.S. Abdou, K.S. Nagy, M.Z. Elsabee, Extraction and characterization of chitin and chitosan from local sources, *Bioresour. Technol.* 99 (2008) 1359-1367.

- [20] J. Majtán, K. Bíliková, O. Markovič, J. Gróf, G. Kogan, J. Šimúth, Isolation and characterization of chitin from bumblebee (*Bombus terrestris*), *Int. J. Biol. Macromol.* 40 (2007) 237-241.
- [21] M. Islam, S.M. Masum, M.M. Rahman, M. Molla, A. Islam, A. Shaikh, S. Roy, Preparation of Chitosan from Shrimp Shell and Investigation of Its Properties, *Int. J. Basic Appl. Sci.* 11 (2011) 77-80.
- [22] E.S. Abdou, K.S.A. Nagy, M.Z. Elsabee, Extraction and characterization of chitin and chitosan from local sources, *Bioresour. Technol.* 99 (2008) 1359-1367.
- [23] A.E. De Salamanca, Y. Diebold, M. Calonge, C. García-Vazquez, S. Callejo, A. Vila, M.J. Alonso, Chitosan nanoparticles as a potential drug delivery system for the ocular surface: toxicity, uptake mechanism and in vivo tolerance, *Invest. Ophthalmol. Vis. Sci.* 47 (2006) 1416-1425.
- [24] S. Cohen, H. Bernstein, *Microparticulate systems for the delivery of proteins and vaccines*, CRC Press 1996.
- [25] R.C. Doijad, D.S. Bhambere, F.V. Manvi, N.V. Deshmukh, Formulation and characterization of vesicular drug delivery system for anti-HIV drug, *J. Global Pharma. Technol.* 1 (2009) 94-100.
- [26] P. Costa, J.M.S. Lobo, Modeling and comparison of dissolution profiles, *Euro. J. Pharma. Sci.* 13 (2001) 123-133.
- [27] R. Pandey, Z. Ahmad, S. Sharma, G. Khuller, Nano-encapsulation of azole antifungals: potential applications to improve oral drug delivery, *Int. J. Pharmaceut.* 301 (2005) 268-276.
- [28] B. Saparia, R. Murthy, A. Solanki, Preparation and evaluation of chloroquine phosphate microspheres using cross-linked gelatin for long-term drug delivery, *Indian J. Pharm. Sci.* 64 (2002) 48-52.

- [29] S. Haznedar, B. Dortunc, Preparation and in vitro evaluation of Eudragit microspheres containing acetazolamide, *Int. J. Pharmaceut.* 269 (2004) 131-140.
- [30] T. Higuchi, Mechanism of sustained-action medication. Theoretical analysis of rate of release of solid drugs dispersed in solid matrices, *J. Pharma. Sci.* 52 (1963) 1145-1149.
- [31] S. Sun, N. Liang, H. Yamamoto, Y. Kawashima, F. Cui, P. Yan, pH-sensitive poly (lactide-co-glycolide) nanoparticle composite microcapsules for oral delivery of insulin, *Int. J. Nanomedicine* 10 (2015) 3489-3498.
- [32] S. Dash, P.N. Murthy, L. Nath, P. Chowdhury, Kinetic modeling on drug release from controlled drug delivery systems, *Acta Pol Pharm* 67(3) (2010) 217-23.
- [33] H.K. Shaikh, R. Kshirsagar, S. Patil, Mathematical models for drug release characterization: a review, *WJPPS* 4 (2015) 324-338.
- [34] J.P. Ruparelia, A.K. Chatterjee, S.P. Duttgupta, S. Mukherji, Strain specificity in antimicrobial activity of silver and copper nanoparticles, *Acta biomater.* 4(3) (2008) 707-716.
- [35] R. Jones, A. Barry, T. Gavan, J. Washington, Susceptibility tests: microdilution and macrodilution broth procedures, *Manual of clinical microbiology*, 4th ed. American Society for Microbiology, Washington, DC (1985) 972-977.
- [36] M. Kaya, T. Baran, S. Erdoğan, A. Menteş, M.A. Özusağlam, Y.S. Çakmak, Physicochemical comparison of chitin and chitosan obtained from larvae and adult Colorado potato beetle (*Leptinotarsa decemlineata*), *Mater. Sci. Eng. C.* 45 (2014) 72-81.
- [37] M. Kaya, N. Bağrıaçık, O. Seyyar, T. Baran, Comparison of chitin structures derived from three common wasp species (*Vespa crabro* Linnaeus, 1758, *Vespa orientalis* Linnaeus, 1771 and *Vespula germanica* (Fabricius, 1793)), *Arch. insect Biochem. Physiol.* 89 (2015) 204-217.

- [38] M. Kaya, M.G. Halıcı, F. Duman, S. Erdoğan, T. Baran, Characterisation of α -chitin extracted from a lichenised fungus species *Xanthoria parietina*, *Nat. Prod. Res.* 29 (2015) 1280-1284.
- [39] M. Kaya, M. Karaarslan, T. Baran, E. Can, G. Ekemen, B. Bitim, F. Duman, The quick extraction of chitin from an epizoic crustacean species (*Chelonibia patula*), *Nat. Prod. Res.* 28 (2014) 2186-2190.
- [40] M. Kaya, T. Baran, I. Saman, M. Asan Ozusaglam, Y.S. Cakmak, A. Menteş, Physicochemical characterization of chitin and chitosan obtained from resting eggs of *Ceriodaphnia quadrangula* (Branchiopoda: Cladocera: Daphniidae), *J. Crustacean Biol.* 34 (2014) 283-288.
- [41] M. Kaya, K.Ö. Tozak, T. Baran, G. Sezen, I. Sargin, Natural porous and nano fiber chitin structure from *Gammarus argaeus* (Gammaridae Crustacea), *Excli J.* 12 (2013) 503-510.
- [42] S. Chatterjee, M. Adhya, A. Guha, B. Chatterjee, Chitosan from *Mucor rouxii*: production and physico-chemical characterization, *Process Bioch.* 40 (2005) 395-400.
- [43] R. Jayakumar, M. Prabakaran, R. Reis, J. Mano, Graft copolymerized chitosan—present status and applications, *Carbohydr. Polym.* 62 (2005) 142-158.
- [44] S. Ifuku, R. Nomura, M. Morimoto, H. Saimoto, Preparation of chitin nanofibers from mushrooms, *Materials* 4 (2011) 1417-1425.
- [45] Y. Wang, Y. Chang, L. Yu, C. Zhang, X. Xu, Y. Xue, Z. Li, C. Xue, Crystalline structure and thermal property characterization of chitin from Antarctic krill (*Euphausia superba*), *Carbohydr. Polym.* 92 (2013) 90-97.
- [46] M.-T. Yen, J.-H. Yang, J.-L. Mau, Physicochemical characterization of chitin and chitosan from crab shells, *Carbohydr. Polym.* 75 (2009) 15-21.

- [47] W. Sajomsang, P. Gonil, Preparation and characterization of α -chitin from cicada sloughs, *Mat. Sci. Eng. C* 30 (2010) 357-363.
- [48] L. Zelencova, S. Erdoğan, T. Baran, M. Kaya, Chitin extraction and chitosan production from Chilopoda (*Scolopendra cingulata*) with identification of physicochemical properties, *Polym. Sci. Ser. A* 57 (2015) 437-444.
- [49] M. Kaya, T. Baran, M. Asan-Ozusaglam, Y.S. Cakmak, K.O. Tozak, A. Mol, A. Mentés, G. Sezen, Extraction and characterization of chitin and chitosan with antimicrobial and antioxidant activities from cosmopolitan Orthoptera species (Insecta), *Biotechnol. Bioprocess Eng.* 20 (2015) 168-179.
- [50] M. Kaya, O. Seyyar, T. Baran, T. Turkes, Bat guano as new and attractive chitin and chitosan source, *Front. Zoology* 11 (2014) 59-69.
- [51] M. Kaya, Y.S. Cakmak, T. Baran, M. Asan-Ozusaglam, A. Mentés, K.O. Tozak, New chitin, chitosan, and O-carboxymethyl chitosan sources from resting eggs of *Daphnia longispina* (Crustacea); with physicochemical characterization, and antimicrobial and antioxidant activities, *Biotechnol. Bioprocess Eng.* 19 (2014) 58-69.
- [52] M. AbdElhady, Preparation and characterization of chitosan/zinc oxide nanoparticles for imparting antimicrobial and UV protection to cotton fabric, *Int. J. Carbohydr. Chem.* 2012 (2012) 1-10.
- [53] L.-H. Li, J.-C. Deng, H.-R. Deng, Z.-L. Liu, L. Xin, Synthesis and characterization of chitosan/ZnO nanoparticle composite membranes, *Carbohydr. Res.* 345 (2010) 994-998.
- [54] T.A. Khan, K.K. Peh, H.S. Ch'ng, Reporting degree of deacetylation values of chitosan: the influence of analytical methods, *J Pharm Pharmaceut Sci* 5 (2002) 205-212.
- [55] V. Kestens, G. Roebben, J. Herrmann, Å. Jämting, V. Coleman, C. Minelli, C. Clifford, P.-J. De Temmerman, J. Mast, L. Junjie, Challenges in the size analysis of a silica

nanoparticle mixture as candidate certified reference material, *J. Nanopart. Res.* 18 (2016) 171.

[56] R.J. Hunter, *Zeta potential in colloid science: principles and applications*, Academic press, 2013.

[57] R.H. Muller, C. Jacobs, O. Kayser, Nanosuspensions as particulate drug formulations in therapy. Rationale for development and what we can expect for the future, *Adv Drug Deliv Rev* 47 (2001) 3-19.

[58] J.-U.A. Junghanns, R.H. Müller, Nanocrystal technology, drug delivery and clinical applications, *Int. J. Nanomedicine* 3 (2008) 295-309.

[59] E. Bahreini, K. Aghaiypour, R. Abbasalipourkabar, A.R. Mokarram, M.T. Goodarzi, M. Saidijam, Preparation and nanoencapsulation of l-asparaginase II in chitosan-tripolyphosphate nanoparticles and in vitro release study, *Nanoscale Res. Lett.* 9 (2014) 340.

[60] Z. Sobhani, S.M. Samani, H. Montaseri, E. Khezri, Nanoparticles of Chitosan Loaded Ciprofloxacin: Fabrication and Antimicrobial Activity, *Adv. Pharm. Bull.* 7 (2017) 427-432.

[61] A. Srinatha, J. Pandit, S. Singh, Ionic cross-linked chitosan beads for extended release of ciprofloxacin: in vitro characterization, *Indian journal of pharmaceutical sciences* 70(1) (2008) 16.

[62] W.-L. Du, S.-S. Niu, Y.-L. Xu, Z.-R. Xu, C.-L. Fan, Antibacterial activity of chitosan tripolyphosphate nanoparticles loaded with various metal ions, *Carbohydr. Polym.* 75 (2009) 385-389.

[63] P. Buri, E. Doelker, Formulation des comprimés à libération prolongée II. Matrices hydrophiles, *Pharm. Acta Helv* 55 (1980) 189-197.

[64] S.K. Ei-Arini, H. Leuenberger, Modelling of drug release from polymer matrices: Effect of drug loading, *Int. J. Pharmaceut.* 121 (1995) 141-148.

- [65] C.G. Varelas, D.G. Dixon, C.A. Steiner, Zero-order release from biphasic polymer hydrogels, *J. Control. Release.* 34 (1995) 185-192.
- [66] N. Mulye, S. Turco, A simple model based on first order kinetics to explain release of highly water soluble drugs from porous dicalcium phosphate dihydrate matrices, *Drug dev. Ind. Pharm.* 21 (1995) 943-953.
- [67] T. Higuchi, Rate of release of medicaments from ointment bases containing drugs in suspension, *J. Pharma. Sci.* 50 (1961) 874-875.
- [68] R.W. Korsmeyer, R. Gurny, E. Doelker, P. Buri, N.A. Peppas, Mechanisms of solute release from porous hydrophilic polymers, *Int. J. Pharmaceut.* 15 (1983) 25-35.
- [69] N. Irene, K. Sasikanth, Preparation and in vitro evaluation of rosiglitazone maleate bi layered bioadhesive floating tablets, *J Chem Pharm Res* 3 (2011) 140-9.
- [70] H. Tang, P. Zhang, T.L. Kieft, S.J. Ryan, S.M. Baker, W.P. Wiesmann, S. Rogelj, Antibacterial action of a novel functionalized chitosan-arginine against Gram-negative bacteria, *Acta Biomater.* 6 (2010) 2562-2571.
- [71] I. Helander, E.-L. Nurmiäho-Lassila, R. Ahvenainen, J. Rhoades, S. Roller, Chitosan disrupts the barrier properties of the outer membrane of Gram-negative bacteria, *Int. J. Food microbiol.* 71 (2001) 235-244.
- [72] M. Azhdarzadeh, F. Lotfipour, P. Zakeri-Milani, G. Mohammadi, H. Valizadeh, Anti-bacterial performance of azithromycin nanoparticles as colloidal drug delivery system against different gram-negative and gram-positive bacteria, *Advanced pharmaceutical bulletin* 2(1) (2012) 17.
- [73] F. Fawaz, F. Bonini, J. Maugein, A. Lagueny, Ciprofloxacin-loaded polyisobutylcyanoacrylate nanoparticles: pharmacokinetics and in vitro antimicrobial activity, *International journal of pharmaceutics* 168(2) (1998) 255-259.

- [74] A.J. Huh, Y.J. Kwon, "Nanoantibiotics": a new paradigm for treating infectious diseases using nanomaterials in the antibiotics resistant era, *Journal of controlled release* 156(2) (2011) 128-145
- [75] F.R. Tamara, C. Lin, F.-L. Mi, Y.-C. Ho, Antibacterial effects of chitosan/cationic peptide nanoparticles, *Nanomaterials* 8(2) (2018) 88.
- [76] L. Qi, Z. Xu, X. Jiang, C. Hu, X. Zou, Preparation and antibacterial activity of chitosan nanoparticles, *Carbohydr. Res.* 339 (2004) 2693-2700.
- [77] M. Banoee, S. Seif, Z.E. Nazari, P. Jafari-Fesharaki, H.R. Shahverdi, A. Moballegh, K.M. Moghaddam, A.R. Shahverdi, ZnO nanoparticles enhanced antibacterial activity of ciprofloxacin against *Staphylococcus aureus* and *Escherichia coli*, *J. Biomed. Mater. Res. B.* 93 (2010) 557-561.
- [78] H. No, N. Park, S. Lee, H. Hwang, S. Meyers, Antibacterial activities of chitosans and chitosan oligomers with different molecular weights on spoilage bacteria isolated from tofu, *J. Food Sci.* 67 (2002) 1511-1514.

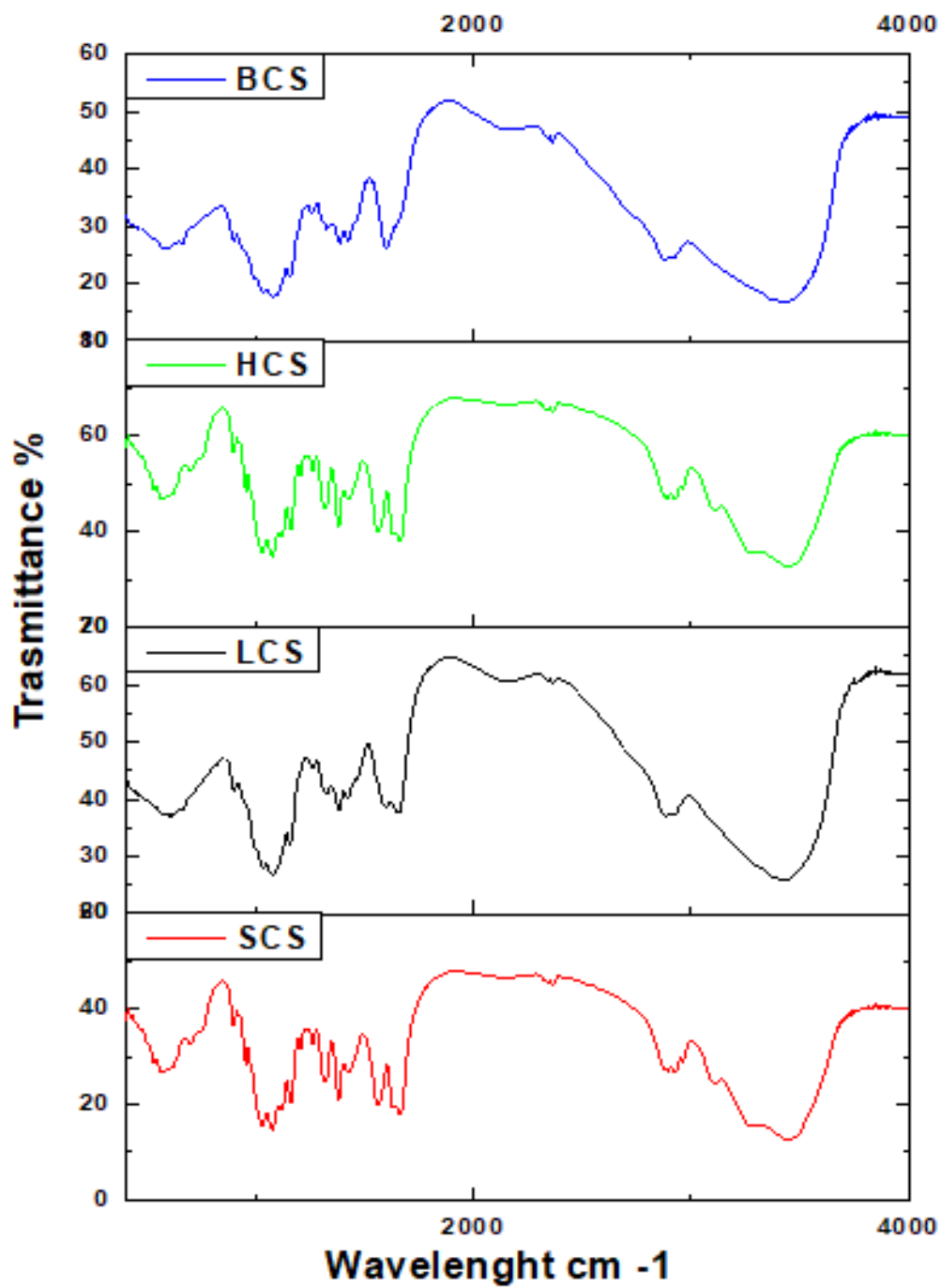


Figure 1: FTIR analysis for BCS, HCS, LCS, and SCS

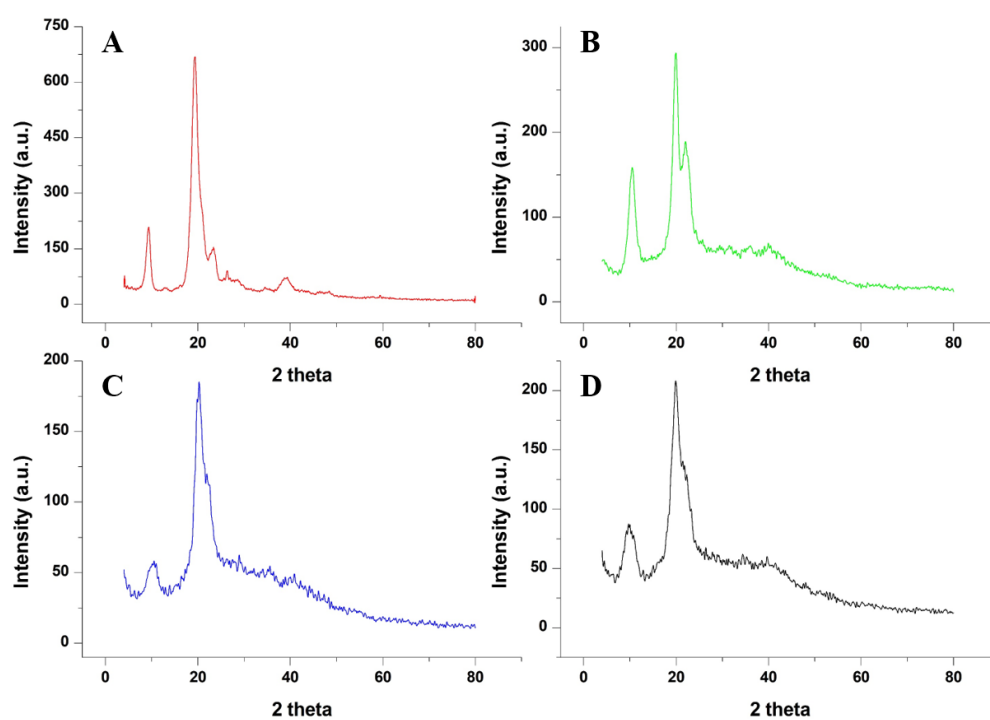


Figure 2: XRD for (A) LCS, (B) BCS, (C) HCS, and (D) SCS.

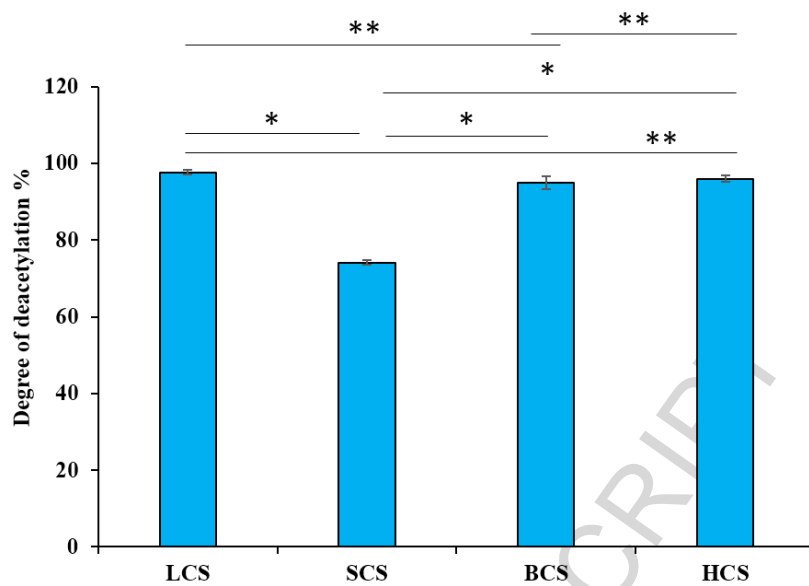


Figure 3: Degree of deacetylation % of chitosan from different sources. Results were expressed as average arithmetic mean. Error bars represent \pm SD. One-way ANOVA was used, and statistical analysis significance was observed ($*0.05 \leq P \leq 0.001$, and $**P \leq 1$). Statistical analysis was done using Statistical Package for Social Sciences (SPSS).

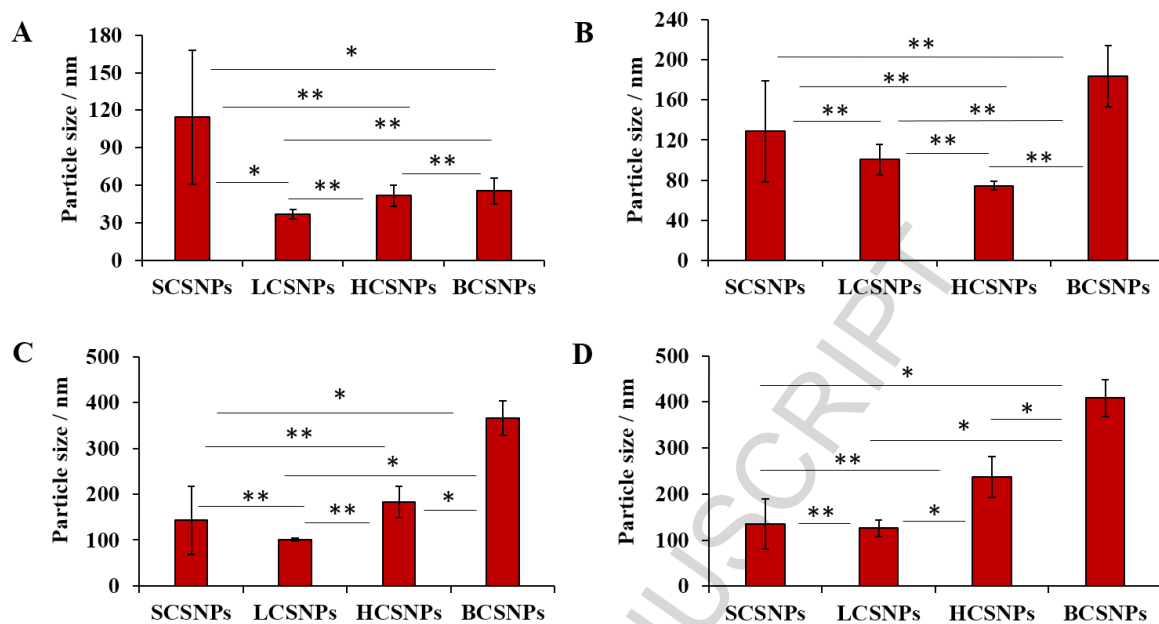


Figure 4: Effect of homogenization time on the particle size distribution of chitosan-based nanoparticles from SCSNPs, LCSNPs, HCSNPs, and BCSNPs at pH = 3.5 (A) 30 min, (B) 60 min, (C) 90 min, and (D) 120 min. Results were expressed as average arithmetic mean. Error bars represent \pm SD. One-way ANOVA was used, and statistical analysis significance was observed ($0.05 \leq P \leq 0.001$, and $**P \leq 1$). Statistical analysis was done using Statistical Package for Social Sciences (SPSS).

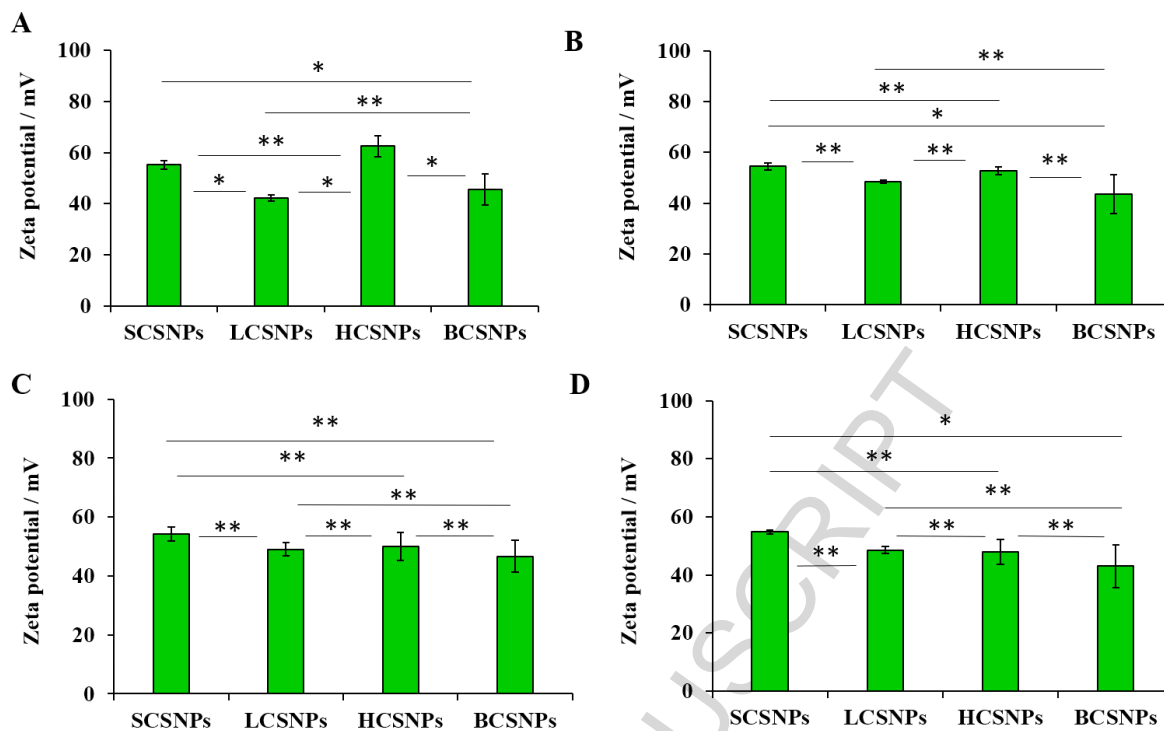


Figure 5: Effect of homogenization time on the Zeta potential of chitosan-based nanoparticles from SCSNPs, LCSNPs, HCSNPs, and BCSNPs at pH = 3.5 (A) 30 min, (B) 60 min, (C) 90 min, and (D) 120 min. Results were expressed as average arithmetic mean. Error bars represent \pm SD. One-way ANOVA was used, and statistical analysis significance was observed (* $P \leq 0.05$, and ** $P > 0.05$). Statistical analysis was done using Statistical Package for Social Sciences (SPSS).

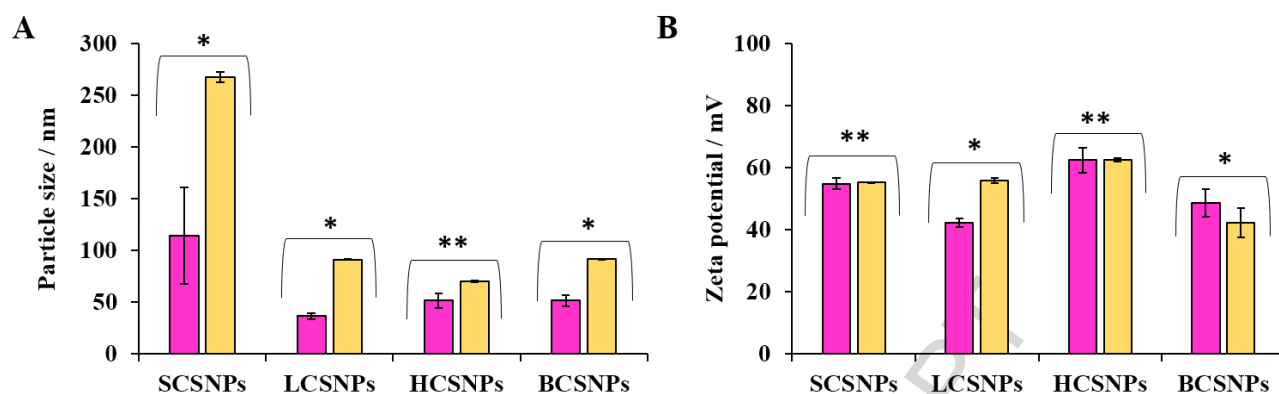


Figure 6: (A) Particle size distribution, and (B) Zeta potential of CSNPs before drug loading (BDL) and after drug loading (ADL) from different sources. Results were expressed as average arithmetic mean. Error bars represent \pm SD. Paired t-test was used, and statistical analysis significance was observed where $*P \leq 0.05$. Statistical analysis was done using Statistical Package for Social Sciences (SPSS).

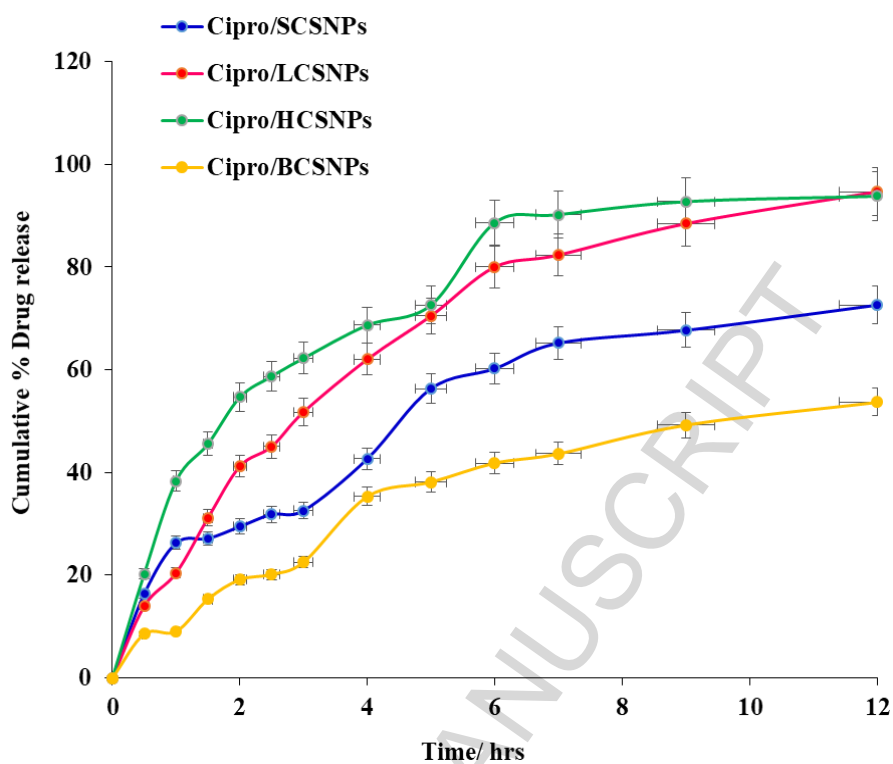


Figure 7: In vitro drug release profile of ciprofloxacin-based chitosan nanoparticles from different sources. Results were expressed as average arithmetic mean. Error bars represent \pm SD.

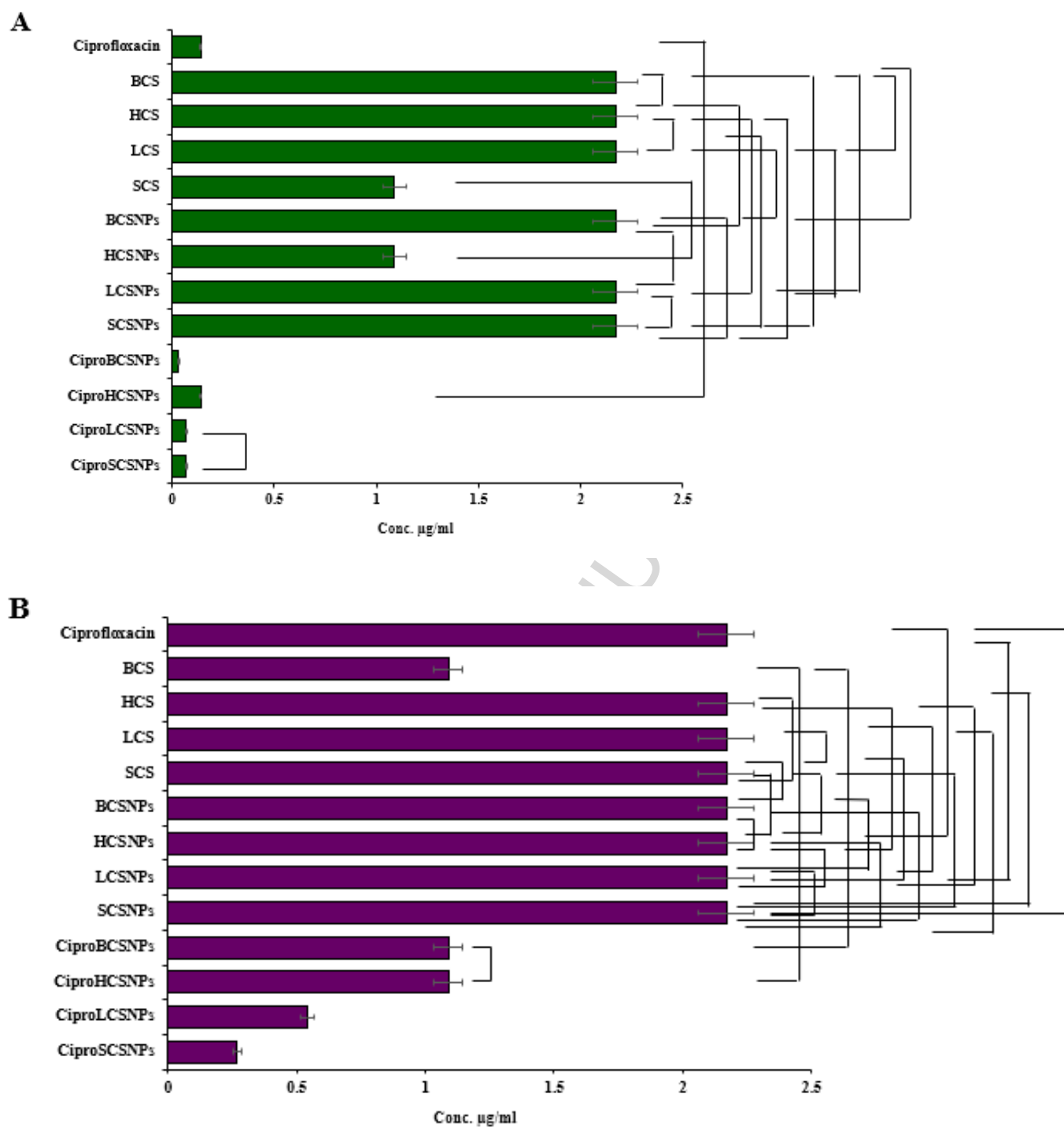


Figure 8: MIC Concentration/ μg of chitosan sample from different sources against gram positive bacteria (A) MRSA, and (B) *P. aeruginosa*. Results were expressed as average arithmetic mean. Error bars represents $\pm\text{SD}$. One-way ANOVA was used, and statistical analysis significance was observed ($P \leq 0.05$ significant, and $P > 0.05$ non-significant). The figure showed the non-significant relations. Statistical analysis was done using Statistical Package for Social Sciences (SPSS).

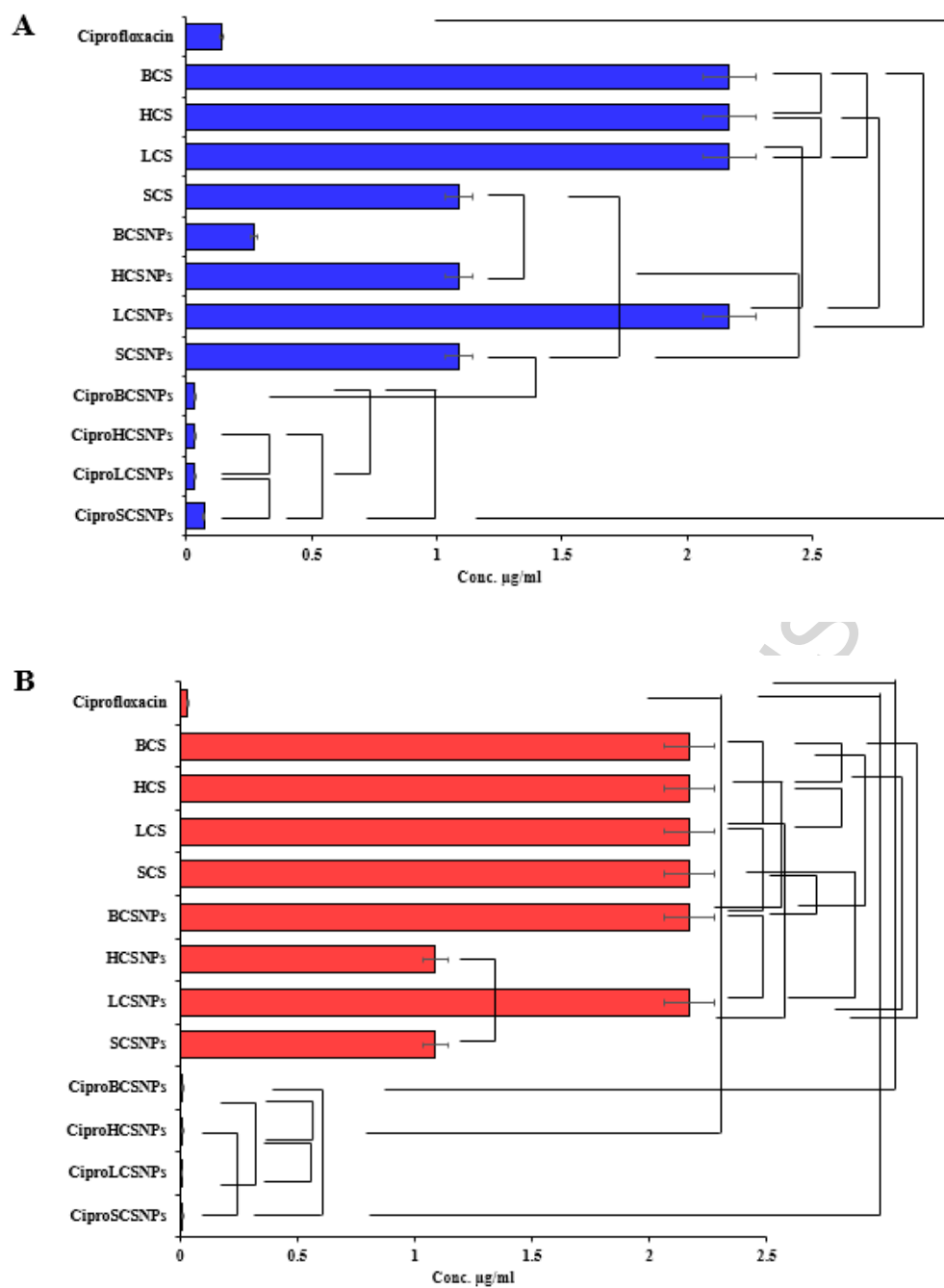


Figure 9: MIC Concentration/ μg of chitosan sample from different sources against gram negative bacteria (A) *B. thuringiensis*, and (B) *E. coli*. Results were expressed as average arithmetic mean. Error bars represents $\pm\text{SD}$. One-way ANOVA was used, and statistical analysis significance was observed ($P \leq 0.05$ significant, and $P > 0.05$ non-significant). The figure showed the non-significant relations. Statistical analysis was done using Statistical Package for Social Sciences (SPSS).